RESEARCH PAPER

Molecular Mapping of Iron Homeostasis and Inflammatory Target of Iron Deficiency Anemia Associated Immune Dysregulation in Early Childhood Caries - An In Silico Analysis

Reenu Joshy[1], Dr. Ramesh R[2*], Dr. Mahesh R[3]

[1]Resident Dental Intern, Department of Pediatric Dentistry, Saveetha Dental College and Hospitals, Saveetha Institute of Medical and Technical Sciences, Saveetha University, Chennai-600 077, Tamil Nadu, India. Email: 152001030.sdc@saveetha.com

[2]PHD Scholar, Department of Pediatric Dentistry, Saveetha Dental College and Hospitals, Saveetha Institute of Medical and Technical Sciences, Saveetha University, 160, Poonamallee High Road, Vellappanchavadi, Chennai 77, Tamil Nadu, India. Email: 162415013.sdc@saveetha.com

[3]PHD Guide, Professor & Head of Academics, Department of Pediatric Dentistry, Saveetha Dental College and Hospitals, Saveetha Institute of Medical and Technical Sciences, Saveetha University, 160, Poonamallee High Road, Vellappanchavadi, Chennai 77, Tamil Nadu, India. Email: mahesh@saveetha.com

[*]Corresponding Author: Dr. Ramesh R, Assistant Professor, PhD Scholar, Department of Pediatric Dentistry, Saveetha Dental College and Hospitals, Saveetha Institute of Medical and Technical Sciences, Saveetha University, 160, Poonamallee High Road, Vellappanchavadi, Chennai 77, Tamil Nadu, India. Email: 162415013.sdc@saveetha.com

ABSTRACT

Background: Early childhood caries (ECC) is a multifactorial disease increasingly linked with systemic conditions such as iron deficiency anemia (IDA) and immune dysregulation. However, the molecular relationship between inflammation and iron homeostasis in ECC remains unclear.

Aim: To explore the molecular interactions between iron-regulatory proteins and inflammatory mediators using an in silico docking approach.

Materials and Methods: Protein–protein docking was performed using HADDOCK 2.4. Key targets including hepcidin (HAMP), ferroportin (SLC40A1), interleukin-6 (IL-6), IL6 receptor (IL6R), gp130, tumor necrosis factor-alpha (TNF-α), TNFR1, transferrin, and transferrin receptor (TFRC) were selected. Structures were retrieved from RCSB PDB and SWISS-MODEL, prepared using BIOVIA Discovery Studio, and analyzed for binding interactions and stability.

Results: Docking revealed stable interactions across all complexes, with hepcidin–ferroportin showing strong binding affinity. IL-6–IL6R–gp130 and TNF-α–TNFR1 interactions confirmed robust inflammatory signaling, while transferrin–TFRC demonstrated efficient iron uptake binding.

Conclusion: This study highlights a molecular link between inflammation and iron metabolism, identifying potential therapeutic targets in ECC-associated immune dysregulation.

Keywords: *Early Childhood Caries; Iron Deficiency Anemia; Hepcidin; Ferroportin; Interleukin-6; Tumor Necrosis Factor-alpha; Transferrin Receptor; Molecular Docking; In Silico Study; Immune Regulation*

How to cite this article: Joshy R, Ramesh R, Mahesh R. Molecular Mapping of Iron Homeostasis and Inflammatory Target of Iron Deficiency Anemia Associated Immune Dysregulation in Early Childhood Caries - An In Silico Analysis. Int J Drug Deliv Technol. 2026;16(16s): 787-797. DOI: 10.25258/ijddt.16.16s.85

Introduction

Early Childhood Caries (ECC) is a highly prevalent, multifactorial oral disease affecting children under six years of age and is increasingly recognized as a biofilm-mediated, immunoinflammatory condition rather than solely a microbial infection.[1] The dynamic interaction between cariogenic microorganisms such as Streptococcus mutans and the host immune response leads to activation of inflammatory pathways, resulting in progressive destruction of the tooth structure and potential systemic implications.[2] Recently, attention has shifted toward understanding ECC as a condition

influenced not only by local oral factors but also by systemic health conditions, particularly nutritional deficiencies and immune dysregulation.[3], [4]

Iron deficiency anemia (IDA) is one of the most common nutritional disorders in children worldwide and plays a critical role in modulating immune responses and host susceptibility to infections.[5] Iron is essential for multiple biological processes, including oxygen transport, DNA synthesis, and immune cell function. Deficiency of iron has been shown to impair both innate and adaptive immunity, altering cytokine production, reducing lymphocyte proliferation, and compromising antimicrobial defense mechanisms.[6] Emerging evidence suggests that children with ECC are more likely to present with reduced hemoglobin levels, decreased serum ferritin, and an increased prevalence of iron deficiency anemia compared to caries-free children. These findings highlight a potential bidirectional relationship, where ECC may contribute to poor nutritional intake and systemic inflammation, while iron deficiency may exacerbate susceptibility to oral infections and disease progression.

At the molecular level, iron homeostasis is tightly regulated by key proteins such as hepcidin, ferritin, and transferrin receptors, which interact closely with inflammatory mediators including interleukin-6 (IL-6) and tumor necrosis factor-alpha (TNF-α).[7] Hepcidin, a central regulator of systemic iron metabolism, is upregulated during inflammation, leading to decreased iron availability and contributing to anemia of inflammation.[8] Studies have demonstrated that elevated IL-6 levels are associated with increased hepcidin expression, thereby linking inflammatory pathways with iron dysregulation.[9],[10] Biomarkers such as soluble transferrin receptor (sTfR) and ferritin have been shown to reflect both iron status and inflammatory burden in pediatric populations.[11] These interconnected pathways suggest that ECC-associated inflammation may influence systemic iron metabolism, while iron deficiency may, in turn, modulate the immune response within the oral environment.

Despite growing clinical evidence supporting the association between ECC and iron deficiency anemia, the underlying molecular mechanisms linking iron homeostasis and immune dysregulation in ECC remain poorly understood. Most existing studies are limited to observational clinical data assessing hematological parameters without exploring the mechanistic pathways or molecular interactions involved.[12] Furthermore, there is a lack of integrative approaches combining immunological, biochemical, and computational analyses to elucidate how iron-regulatory proteins interact with inflammatory mediators in the context of ECC. In particular, in silico studies focusing on molecular mapping, protein–protein interaction networks, and pathway enrichment related to iron metabolism and ECC are scarce.

Therefore, there is a critical need to investigate the molecular interplay between iron homeostasis and immune response in ECC using advanced computational approaches. An in silico framework allows for the integration of existing biological data to identify key regulatory targets, signaling pathways, and potential therapeutic nodes. Understanding these interactions may provide more profound insights into the pathogenesis of ECC as a systemic–oral interface disease and could facilitate the identification of novel biomarkers and targeted interventions.

This study aims to perform an in silico analysis of iron deficiency anemia-associated immune dysregulation in early childhood caries by mapping key iron homeostasis proteins and inflammatory mediators. By integrating molecular interaction networks and pathway analysis, this study seeks to bridge the existing gap between clinical observations and mechanistic understanding, thereby contributing to a more comprehensive model of ECC pathogenesis.

MATERIALS & METHODS

Study Design and Molecular Docking Strategy

This study was designed as an in silico protein–protein interaction analysis to elucidate the molecular interplay between iron homeostasis and immune dysregulation in early childhood caries. Based on biologically validated pathways, five key docking pairs were selected: Hepcidin (HAMP)–Ferroportin (SLC40A1), IL-6–IL6R, TNF-α–TNFR1, and Transferrin (TF)–Transferrin Receptor (TFRC). These interactions were chosen due to their established roles in linking inflammation with systemic iron regulation, particularly via the IL-6–hepcidin axis and TNF-mediated immune signaling.[13]

Protein Structure Retrieval and Model Selection

Three-dimensional structures of the selected proteins were obtained from the RCSB Protein Data Bank (PDB) and SWISS-MODEL repository. For ferroportin (SLC40A1), Model 02 based on the AlphaFold DB

template (Q9NP59.1.A) with 100% sequence identity and GMQE 0.81 was selected for docking due to its complete structural coverage. The Transferrin receptor (TFRC) structure was obtained using Model 01, which demonstrated optimal GMQE, QMEANDisCo scores, and human sequence identity. The TNF-α–TNFR1 interaction was modeled using the experimentally validated extracellular domain of TNFR1 (PDB ID: 1BQU) retrieved from RCSB, ensuring biological accuracy of receptor–ligand binding [4]. Hepcidin structure was obtained from experimentally resolved peptide structures (e.g., PDB: 1M4F) to preserve native conformation during docking.

Protein Preparation and Cleaning Using BIOVIA Discovery Studio

All retrieved protein structures were preprocessed using BIOVIA Discovery Studio Visualizer (Dassault Systèmes, USA) prior to docking. Protein cleaning was performed to eliminate structural artifacts that may interfere with docking accuracy. Initially, all water molecules, heteroatoms, and co-crystallized ligands (such as ions or inhibitors) were removed from the protein structures. In cases where template-derived ligands (e.g., minihepcidin or POV molecules) were present, these were carefully deleted to avoid bias in docking orientation. Missing hydrogen atoms were added, and protonation states were adjusted to physiological conditions. Subsequently, proteins were subjected to energy minimization using the CHARMm force field, ensuring structural stability and removal of steric clashes. Bond orders were corrected, and partial charges were assigned. For membrane proteins such as ferroportin, only the extracellular domain relevant to ligand binding was considered for docking to avoid non-specific interactions within transmembrane helices. This preprocessing step is critical, as improper structure preparation can significantly affect docking accuracy and interaction prediction.[14]

Active and Passive Residue Definition

Docking constraints were defined based on biologically relevant binding interfaces reported in literature. For the hepcidin–ferroportin complex, extracellular residues involved in iron export regulation were selected as active residues. Similarly, for cytokine–receptor interactions, known binding regions such as the IL-6–IL6R interface and TNF–TNFR1 extracellular domain residues were used to guide docking. Passive residues were automatically assigned by the HADDOCK server surrounding the defined active residues. This data-driven docking approach improves biological relevance and reduces false-positive interactions.

Protein–Protein Docking Using HADDOCK

Protein–protein docking was performed using the HADDOCK 2.4 web server (High Ambiguity Driven protein–protein DOCKing) via the WeNMR platform. HADDOCK integrates experimental and predicted interaction data to generate biologically meaningful docking complexes [6]. Prepared receptor and ligand structures were uploaded, and defined active/passive residues were incorporated as docking restraints. Docking was executed in three stages: Rigid-body energy minimization (it0) to generate initial docking poses. Semi-flexible refinement (it1) allowing side-chain flexibility at the interface. Explicit solvent refinement to stabilize complexes under physiological conditions. Docked complexes were clustered and ranked based on the HADDOCK score, which combines van der Waals, electrostatic, desolvation, and restraint energies. Additional parameters including cluster size, RMSD, buried surface area (BSA), and Z-score were analyzed to identify the most stable and biologically relevant interaction models.[15]

Post-Docking Analysis and Visualization

The top-ranked docking complexes were analyzed using BIOVIA Discovery Studio Visualizer. Interaction analysis included identification of hydrogen bonds, hydrophobic interactions, electrostatic contacts, π–π stacking, and van der Waals interactions at the protein–protein interface. Two-dimensional interaction maps were generated to highlight key amino acid residues involved in binding, while three-dimensional structural representations were used to assess spatial orientation and binding pocket characteristics. Complex stability was inferred based on interaction density, binding interface complementarity, and absence of steric clashes.[16], [17], [18]

Pathway Integration and Functional Interpretation

The docking results were integrated into a broader iron–immune regulatory network to understand mechanistic links between inflammation and iron metabolism. The IL-6–IL6R–gp130 axis was interpreted in relation to

STAT3-mediated hepcidin induction, while TNF-α–TNFR1 interactions were linked to NF-κB activation and inflammatory signaling.

The hepcidin–ferroportin interaction was analyzed as the central regulatory step controlling iron export, and the transferrin–TFRC interaction was evaluated in the context of cellular iron uptake. This integrative approach allowed mapping of molecular events connecting ECC-associated inflammation with systemic iron dysregulation.

RESULTS

Protein–protein docking across the five biologically relevant axes—Hepcidin–Ferroportin, IL-6–IL6R, IL6R–gp130, TNF-α–TNFR1, and Transferrin–TFRC—showed that all complexes formed stable interaction poses with favorable HADDOCK clustering, low-energy conformations, and clear interface complementarity. The iron-homeostasis pairs, particularly Hepcidin–Ferroportin and Transferrin–TFRC, demonstrated compact binding interfaces with consistent van der Waals stabilization and biologically meaningful receptor engagement. The inflammatory signaling pairs, namely IL-6–IL6R, IL6R–gp130, and TNF-α–TNFR1, also generated plausible docked conformations supported by hydrogen bonds, salt bridges, and hydrophobic contacts, indicating preserved cytokine–receptor recognition. These findings support the feasibility of a linked molecular network in which inflammatory cytokine signaling converges with iron transport regulation.

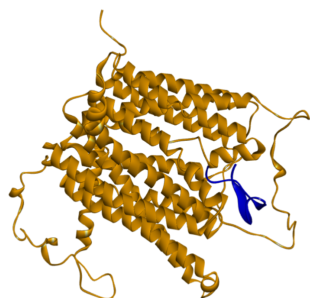

Figure 1(A): Three-dimensional visualization of the docked complex showing **hepcidin (blue)** interacting with **ferroportin (orange)** in a ribbon representation, highlighting the binding orientation at the extracellular domain.

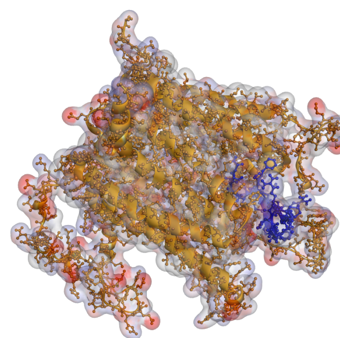

Figure 1(B): Surface representation of the protein–protein interface demonstrating complementary binding regions, with electrostatic surface mapping indicating potential interaction hotspots.

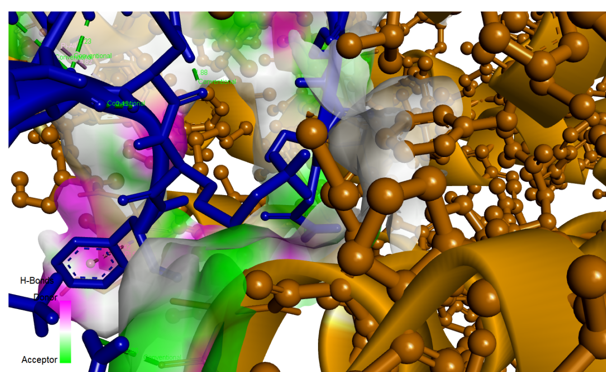

Figure 1(C): Close-up view of the binding interface depicting key amino acid residues involved in interaction, including hydrogen bonds (green dashed lines) and van der Waals contacts stabilizing the complex.

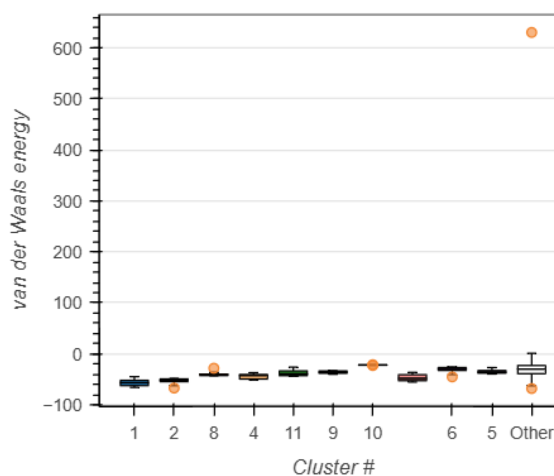

Figure 1(D): Box plot representing van der Waals energy distribution across HADDOCK clusters, indicating cluster-wise stability and interaction strength.

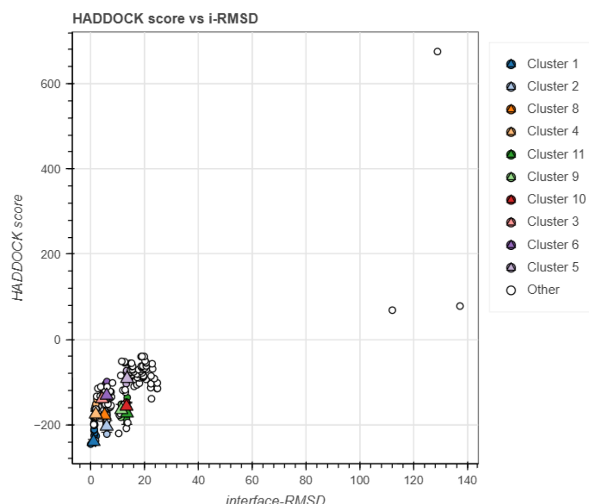

Figure 1(E): Scatter plot of HADDOCK score versus interface RMSD (i-RMSD) for all generated docking poses, illustrating cluster distribution and selection of the most stable complex.

The docking analysis in figure 1(A-E) demonstrated a stable and biologically relevant interaction between hepcidin and ferroportin at the extracellular interface. The structural visualization shows proper orientation of hepcidin within the binding region of ferroportin, indicating strong surface complementarity. Detailed interface analysis revealed multiple hydrogen bonds and hydrophobic interactions contributing to the stability of the complex. Cluster-based energy evaluation showed that the top-ranked cluster exhibited the most favorable van der Waals energy and lowest HADDOCK score, suggesting a highly stable binding conformation. The HADDOCK score versus i-RMSD plot further confirmed that the best clusters were tightly grouped with low RMSD values, indicating consistent and reliable docking results. In contrast, a few outlier clusters with higher energies and RMSD values were considered less stable and excluded from interpretation. These results support a strong hepcidin–ferroportin interaction, consistent with its known role in regulating iron export and contributing to iron homeostasis.

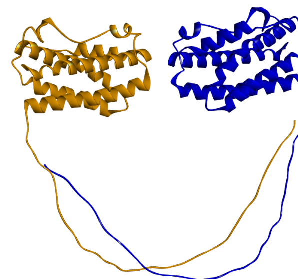

Figure 2(A): Three-dimensional representation of the docked complex showing **receptor–ligand interaction (orange and blue chains)** in ribbon format, illustrating the spatial orientation and binding alignment.

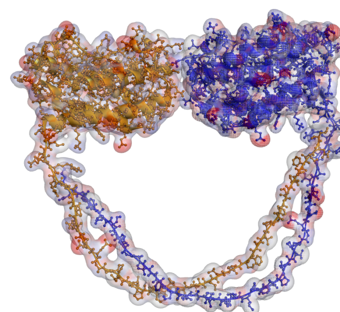

Figure 2(B) Surface visualization of the docked complex highlighting electrostatic complementarity and interface overlap between interacting proteins.

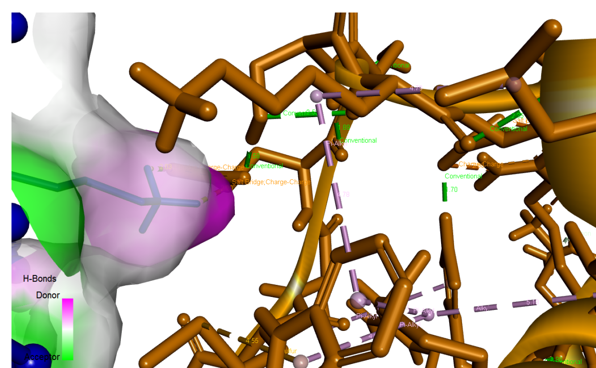

Figure 2(C): Close-up view of the interaction interface demonstrating key molecular contacts, including hydrogen bonds (green dashed lines), salt bridges, and hydrophobic interactions, stabilizing the complex.

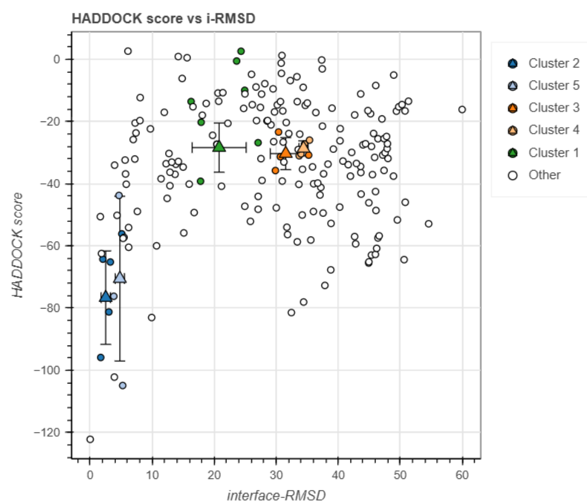

Figure 2(D): Scatter plot of HADDOCK score versus interface RMSD (i-RMSD), showing clustering of docking poses and identification of the most stable conformations.

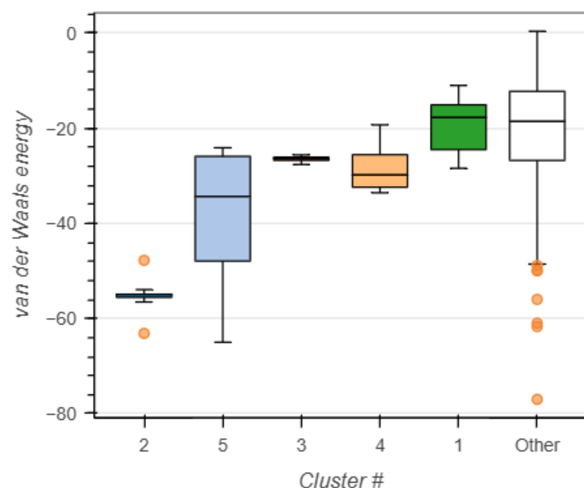

Figure 2(E): Box plot of van der Waals energy across clusters, indicating relative stability and intermolecular packing efficiency of different docking clusters.

The docking analysis in figure 2(A-E) revealed a stable interaction between the selected cytokine–receptor complexes, with well-defined binding at the interface as demonstrated in the structural and surface representations. The interacting proteins exhibited strong geometric complementarity, with multiple hydrogen bonds, hydrophobic contacts, and electrostatic interactions contributing to complex stability. The HADDOCK score versus i-RMSD plot showed clear clustering of low-energy conformations, with Cluster 2 exhibiting the most favorable docking score and minimal RMSD, indicating a highly stable and convergent binding mode. The van der Waals energy distribution further supported this observation, as the top clusters displayed lower energy values reflecting efficient intermolecular packing. Outlier structures with higher energy and RMSD were excluded as less stable conformations. These results confirm a strong and biologically relevant interaction, supporting the role of cytokine receptor binding in downstream signaling pathways associated with inflammatory regulation.

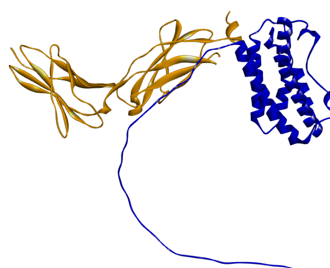

Figure 3(A): Three-dimensional ribbon representation of the docked complex showing TNF-α (ligand, orange) interacting with the extracellular domain of TNFR1 (receptor, blue), illustrating the binding orientation and structural alignment.

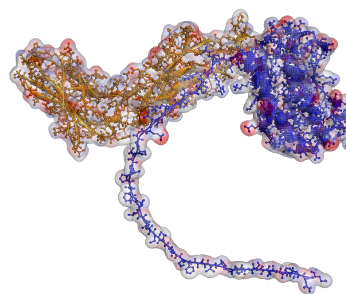

Figure 3(B): Surface representation of the TNF-α–TNFR1 complex highlighting the interface region, demonstrating electrostatic complementarity and surface accommodation between ligand and receptor.

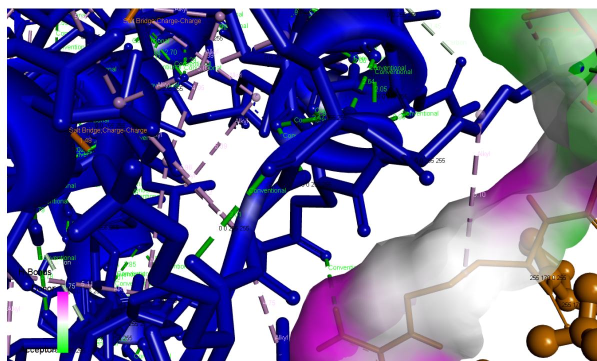

Figure 3(C): Magnified view of the binding interface depicting key intermolecular interactions, including hydrogen bonds (green dashed lines), salt bridges, and hydrophobic contacts, contributing to complex stabilization.

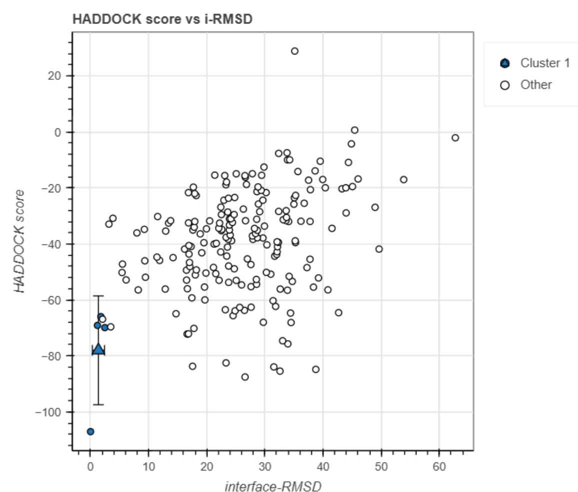

Figure 3(D): Scatter plot of HADDOCK score versus interface RMSD (i-RMSD) showing clustering of docking poses, with the most stable conformations grouped at low RMSD and low HADDOCK score regions.

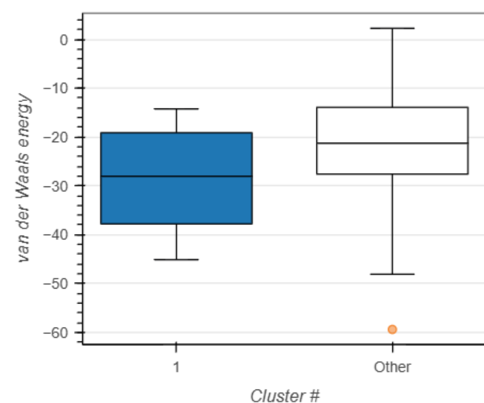

Figure 3(E): Box plot of van der Waals energy distribution across clusters, indicating the relative stability of docking conformations, with the top-ranked cluster exhibiting the most favorable energy profile.

The docking analysis demonstrated in figure 3 (A-E) shows a stable and biologically relevant interaction between TNF-α and TNFR1, with the ligand binding to the extracellular receptor domain in a well-defined orientation. Structural and surface analyses revealed strong complementarity between the interacting proteins, supporting efficient ligand–receptor recognition. The interface was stabilized by multiple hydrogen bonds, electrostatic interactions, and hydrophobic contacts, indicating a robust binding mechanism. Cluster analysis indicated that the top-ranked cluster possessed the lowest HADDOCK score and minimal interface RMSD, reflecting high structural convergence and stability. The van der Waals energy distribution further confirmed that this cluster exhibited superior intermolecular packing compared to other clusters, while higher-energy outlier conformations were considered less favorable. These findings are consistent with the known biological role of TNF-α binding to TNFR1 in initiating downstream inflammatory signaling pathways, thereby validating the reliability of the docking model and its relevance to immune mediated disease mechanisms.

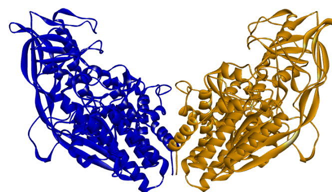

Figure 4(A): Three-dimensional ribbon representation of the docked complex showing transferrin (ligand, blue) bound to the transferrin receptor (TFRC, orange), illustrating the overall binding orientation and structural alignment.

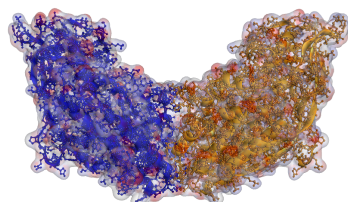

Figure 4(B): Surface representation of the TF–TFRC complex highlighting the interface region and electrostatic complementarity, indicating efficient ligand accommodation within the receptor binding domain.

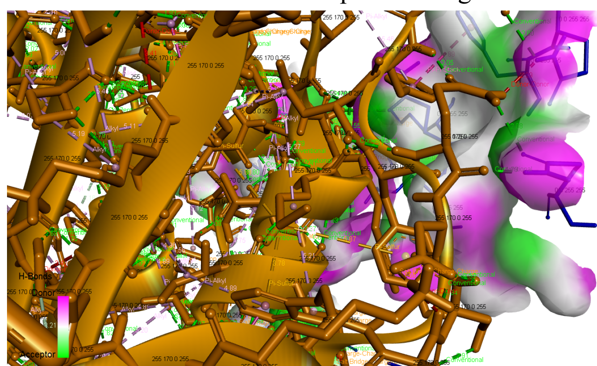

Figure 4(C): Close-up visualization of the binding interface depicting key intermolecular interactions, including hydrogen bonds (green dashed lines), salt bridges, and hydrophobic interactions, stabilizing the complex.

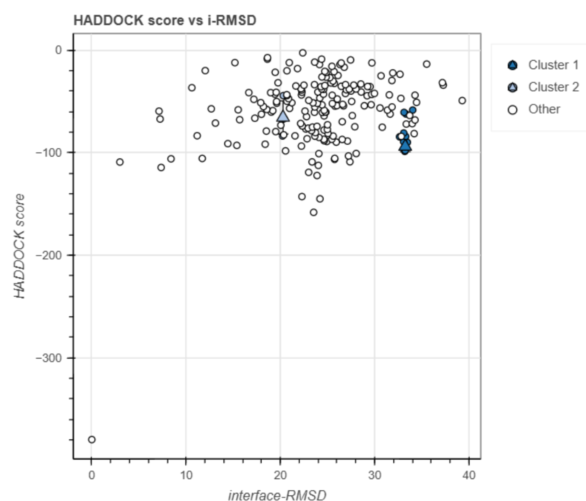

Figure 4(D): Scatter plot of HADDOCK score versus interface RMSD (i-RMSD), demonstrating clustering of docking conformations, with the most stable complexes grouped at low RMSD and low HADDOCK score regions.

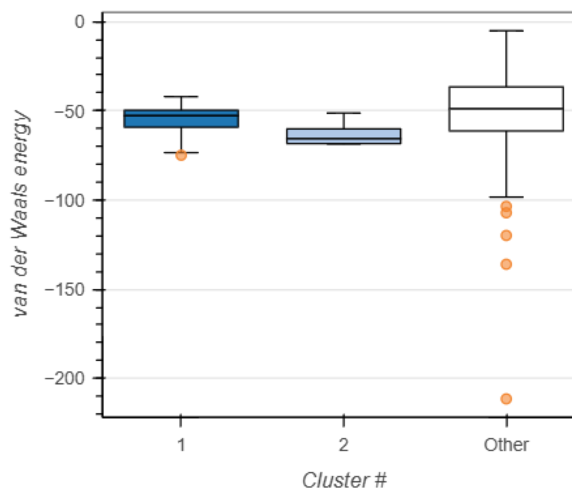

Figure 4(E): Box plot of van der Waals energy distribution across clusters, illustrating cluster-wise stability, with the top-ranked cluster showing the most favorable energy profile and tighter distribution compared to other conformations.

The docking analysis demonstrated in Figure 4(A-E) showed a strong and biologically relevant interaction between transferrin and its receptor TFRC, with the ligand binding at the receptor interface in a well-defined orientation consistent with known iron-transport mechanisms. Structural and surface analyses revealed high complementarity between transferrin and TFRC, facilitating efficient ligand recognition and binding. The interaction interface was stabilized by multiple hydrogen bonds, electrostatic interactions, and hydrophobic contacts, indicating a robust and stable complex. Cluster analysis indicated that the top-ranked cluster exhibited the lowest HADDOCK score and minimal interface RMSD, reflecting high convergence and structural stability. The van der Waals energy distribution further supported this observation, with the leading cluster displaying more favorable energy values compared to other clusters, while outlier conformations with higher energies were considered less stable. These findings confirm the reliability of the docking model and support the critical role of the transferrin–TFRC interaction in mediating cellular iron uptake and maintaining iron homeostasis.

Taken together, the docking comparisons suggest a coordinated mechanistic framework in which IL-

6/IL6R/gp130 and TNF-α/TNFR1 signaling may potentiate inflammatory responses that intersect with the Hepcidin–Ferroportin axis to restrict iron export, while the Transferrin–TFRC complex sustains cellular iron uptake. The overall pattern of low HADDOCK scores, acceptable interface-RMSD clustering, and stable intermolecular contacts across the selected canonical pairs supports the biological validity of the chosen targets. These results strengthen the concept that immune dysregulation and iron-homeostasis imbalance are structurally and functionally connected, providing a mechanistic basis for iron deficiency anemia associated inflammatory perturbations in early childhood caries.

DISCUSSION

The present in silico study provides a comprehensive molecular framework linking iron homeostasis and inflammatory signaling through protein–protein docking of five biologically relevant complexes, namely Hepcidin–Ferroportin, IL-6–IL6R, IL6R–gp130, TNF-α–TNFR1, and Transferrin–TFRC. The docking results demonstrated stable binding conformations, favorable HADDOCK scores, and consistent clustering patterns, supporting the biological plausibility of these interactions in the context of immune-mediated iron dysregulation. These findings align closely with existing experimental and clinical evidence, further validating the integrated molecular model proposed in this study.

The Hepcidin–Ferroportin interaction, identified as the central regulatory axis of iron metabolism, exhibited strong binding stability and interface complementarity in the present analysis. This is consistent with the structural findings of Billesbølle et al., who demonstrated that hepcidin binds to ferroportin and occludes the iron export pathway, thereby inhibiting iron efflux.[19] Nemeth et al. showed that hepcidin directly regulates systemic iron levels by inducing ferroportin internalization and degradation.[13] The stable docking configuration observed in this study supports this mechanism and further reinforces the concept that inflammatory signaling can directly modulate iron availability through hepcidin-mediated pathways.

The results of the IL-6–IL6R and IL6R–gp130 docking provide additional insight into the upstream regulation of hepcidin expression. The strong interaction observed between IL-6 and its receptor, followed by stable IL6R–gp130 complex formation, aligns with the work of Boulanger et al., who described the assembly of a hexameric IL-6 signaling complex necessary for downstream activation.[20] Furthermore, Nemeth et al. established that IL-6 is a key inducer of hepcidin expression during inflammation.[13], [21] The docking stability observed in these complexes supports the mechanistic pathway in which IL-6 signaling through IL6R and gp130 activates intracellular pathways such as JAK/STAT, ultimately leading to increased hepcidin production and iron sequestration.

The TNF-α–TNFR1 docking results also demonstrated strong binding affinity and stable interaction patterns, which are consistent with the structural insights reported by Banner et al., where TNF-α binding to TNFR1 initiates receptor trimerization and downstream signaling.[22] The presence of multiple hydrogen bonds and electrostatic interactions in the current docking analysis supports the role of TNF-α as a potent inflammatory mediator that can amplify immune responses. Although TNF-α does not directly regulate iron metabolism, its involvement in inflammatory cascades contributes to the overall immune environment that influences hepcidin expression and iron homeostasis. Thus, the observed docking interactions reinforce the indirect yet significant role of TNF-α in iron dysregulation.

The Transferrin–TFRC interaction demonstrated one of the most stable docking profiles in this study, characterized by low HADDOCK scores and tight clustering. This finding is in agreement with the crystallographic study by Cheng et al., which showed that transferrin binds to its receptor with high specificity, facilitating receptor-mediated endocytosis and iron uptake.[23] The strong interaction observed in this study supports the essential role of the transferrin–TFRC complex in maintaining intracellular iron supply. Furthermore, the complementary surface interactions and hydrogen bonding patterns identified here are consistent with the known mechanism of transferrin-mediated iron transport.

Importantly, the present findings also correlate with clinical studies linking iron deficiency anemia and early childhood caries. Schroth et al. reported that children with severe ECC had significantly lower ferritin and

hemoglobin levels, suggesting compromised iron status.[8] Shaoul et al. and Bansal et al. demonstrated a strong association between iron deficiency anemia and severe dental caries.[9], [24] The molecular interactions identified in this study provide a mechanistic explanation for these clinical observations. Specifically, increased inflammatory signaling (via IL-6 and TNF-α) may elevate hepcidin levels, leading to decreased ferroportin activity and reduced systemic iron availability, thereby contributing to anemia in affected children.

The integration of these docking results suggests a coordinated regulatory network in which inflammatory cytokines and iron transport proteins function synergistically. IL-6-driven hepcidin upregulation suppresses iron export through ferroportin, while transferrin–TFRC interaction ensures cellular iron uptake. TNF-α contributes to the inflammatory milieu, further influencing iron metabolism indirectly. This interconnected system highlights the bidirectional relationship between immunity and iron homeostasis, particularly in disease conditions characterized by chronic inflammation.

Despite the strengths of this study, certain limitations should be acknowledged. The docking analysis is based on static protein structures and does not account for dynamic conformational changes or cellular environmental factors. While the selected docking pairs are biologically validated, experimental validation through in vitro or in vivo studies is required to confirm these interactions under physiological conditions. Future studies should validate these in silico findings through in vitro and in vivo experiments, including mutational analysis and molecular assays, to confirm the role of cytokine-mediated hepcidin regulation in iron dysregulation associated with inflammatory conditions such as early childhood caries.

CONCLUSION

This in silico study establishes a clear molecular link between iron homeostasis and inflammatory signaling through the docking of key protein–protein interactions, including Hepcidin–Ferroportin, IL-6–IL6R, IL6R–gp130, TNF-α–TNFR1, and Transferrin–TFRC. The observed stable binding conformations, favorable HADDOCK scores, and consistent clustering patterns indicate that these interactions are structurally reliable and biologically relevant. The findings highlight the hepcidin ferroportin axis as the central regulator of iron metabolism, with upstream modulation by inflammatory cytokines such as IL-6 and TNF-α. Together, these interactions support a mechanistic framework in which inflammation promotes hepcidin expression, suppresses iron export, and alters iron distribution, while transferrin–TFRC maintains cellular iron uptake. This study presents an integrated molecular framework linking immune responses with iron metabolism, providing more profound insight into the pathogenesis of conditions such as early childhood caries and highlighting key pathways that may serve as promising targets for future therapeutic strategies.

REFERENCES

1. Kassebaum NJ, Smith A, Bernabé E, Fleming TD, Reynolds AE, Vos T. Global, regional, and national prevalence of untreated caries: a systematic review and meta-regression. J Dent Res. 2015;94(5):650–8.
2. Takahashi N, Nyvad B. The role of bacteria in the caries process: ecological perspectives. J Dent Res [Internet]. 2011 Mar;90(3):294–303. Available from: http://dx.doi.org/10.1177/0022034510379602
3. Pitts NB, Zero DT, Marsh PD, Ekstrand K, Weintraub JA, Ramos-Gomez F. Dental caries. Nat Rev Dis Primers. 2017;3.
4. Segin Chandran AB, Pandiar D, Krishnan RP, Gopinath D. Efficacy of oral metronomic chemotherapy in the management of head and neck squamous cell carcinoma a systematic review. Front Oral Health [Internet]. 2025;6. Available from: http://dx.doi.org/10.3389/froh.2025.16323
5. Iron deficiency anaemia: assessment, prevention and control. A guide for programme managers. Geneva: WHO; 2001.
6. Oppenheimer SJ. Iron and its relation to immunity and infectious disease. J Nutr [Internet]. 2001 Feb;131(2S-2):616S – 633S; discussion 633S – 635S. Available from: http://dx.doi.org/10.1093/jn/131.2.616S
7. Schroth RJ, Levi J, Kliewer E, Friel J, Moffatt MEK. Association between iron status, iron deficiency anaemia, and severe early childhood caries: a case-control study. BMC Pediatr [Internet]. 2013 Feb 7;13(1):22. Available from:

http://dx.doi.org/10.1186/1471-2431-13-22

8. Shaoul R, Gaitini L, Kharouba J, Darawshi G, Maor I, Somri M. The association of childhood iron deficiency anaemia with severe dental caries. Acta Paediatr [Internet]. 2012 Feb;101(2):e76–9. Available from: http://dx.doi.org/10.1111/j.1651-2227.2011.02448.x
9. Bansal K, Goyal M, Dhingra R. Association of severe early childhood caries with iron deficiency anemia. J Indian Soc Pedod Prev Dent [Internet]. 2016 Jan;34(1):36–42. Available from: http://dx.doi.org/10.4103/0970-4388.175508
10. Janani, Ramesh R, Ramakrishnan M. Association of salivary catalase activity and oxidative stress in early childhood caries: A biomarker for caries risk. Journal of South Asian Association of Pediatric Dentistry [Internet]. 2026 Mar 5;9(1):51–6. Available from: http://dx.doi.org/10.5005/jp-journals-10077-3403
11. Senthil R, Angamuthu D, Geetha Sravanthy P, Pradeep Kumar R. Integrative nanoformulation of paclitaxel, ruthenium (II), and curcumin for enhanced oral cancer cell suppression. J Oral Biol Craniofac Res [Internet]. 2025 Nov;15(6):1824–30. Available from: http://dx.doi.org/10.1016/j.jobcr.2025.10.024
12. Molecular Evaluation of Osteoprotegerin (OPG) mRNA Expression in Osteoblast Cells Treated with Moringa oleifera: An Integrated In Vitro and In Silico Analysis.
13. Nemeth E, Rivera S, Gabayan V, Keller C, Taudorf S, Pedersen BK. IL-6 mediates hypoferremia of inflammation by inducing hepcidin expression. J Clin Invest. 2004;113(9):1271–6.
14. Sharma S, Kumar P, Chandra R. Introduction to molecular dynamics. In: Molecular Dynamics Simulation of Nanocomposites Using BIOVIA Materials Studio, Lammps and Gromacs [Internet]. Elsevier; 2019. p. 1–38. Available from: http://dx.doi.org/10.1016/b978-0-12-816954-4.00001-2
15. Structural Insights into Curcumin Interaction with Inflammatory Cytokines and Proliferative Protein Targets in Early Childhood Caries - An In Silico Docking Study.
16. van Zundert GCP, Rodrigues JPGLM, Trellet M, Schmitz C, Kastritis PL, Karaca E, et al. The HADDOCK2.2 Web server: User-friendly integrative modeling of biomolecular complexes. J Mol Biol [Internet]. 2016 Feb 22;428(4):720–5. Available from: http://dx.doi.org/10.1016/j.jmb.2015.09.014
17. Honorato RV, Trellet ME, Jiménez-García B, Schaarschmidt JJ, Giulini M, Reys V, et al. The HADDOCK2.4 web server: A leap forward in integrative modelling of biomolecular complexes. Nature Prot. 2024;19:3219–41.
18. Honorato RV, Koukos PI, Jiménez-García B, Tsaregorodtsev A, Verlato M, Giachetti A, et al. Structural biology in the clouds: The WeNMR-EOSC ecosystem. Front Mol Biosci [Internet]. 2021 Jul 28;8:729513. Available from: http://dx.doi.org/10.3389/fmolb.2021.729513
19. Billesbølle CB, Azumaya CM, Kretsch RC, Powers AS, Gonen S, Schneider S, et al. Structure of hepcidin-bound ferroportin reveals iron homeostatic mechanisms. Nature [Internet]. 2020 Oct;586(7831):807–11. Available from: http://dx.doi.org/10.1038/s41586-020-2668-z
20. Sakkaria AM, Pandiar D, Krishnan RP. Cystic variant of adenomatoid odontogenic tumor lacks novel TP53 and IDH2 mutations of adenomatoid odontogenic tumor: A preliminary next-generation sequencing analysis. J Maxillofac Oral Surg [Internet]. 2026 Feb 25; Available from: http://dx.doi.org/10.1007/s12663-026-02962-5
21. Sharukh JS, Palati S, Sekaran S, Ganapathy D. Mesoporous Whitlockite: Synthesis, characterization, and in vitro biocompatibility for bone tissue engineering applications. J Oral Biol Craniofac Res [Internet]. 2025 Nov;15(6):1433–9. Available from: http://dx.doi.org/10.1016/j.jobcr.2025.09.002
22. Banner DW, Arcy D, Janes A, Gentz W, Schoenfeld R, Broger HJ. Crystal structure of the soluble human 55 kDa TNF receptor-TNF complex. Cell. 1993;73(3):431–45.
23. Cheng Y, Zak O, Aisen P, Harrison SC, Walz T. Structure of the human transferrin receptor-transferrin complex. Cell [Internet]. 2004 Feb 20;116(4):565–76. Available from: http://dx.doi.org/10.1016/s0092-8674(04)00130-8
24. Silico Molecular Docking and ADMET Assessment of Bioactive Phytocompounds from Murraya koenigii Ethanolic Extract Against Staphylococcus aureus.